LOS ALAMOS SCIENTIFIC LABORATORY
OF THE UNIVERSITY OF CALIFORNIA o LOS ALAMOS NEW MEXICO

BETA DECAYS AND DELAYED GAMMAS FROM FISSION FRAGMENTS

LEGAL NOTICE

Printed in USA. Price $ 1.25. Available from the

Office of Technical Services
U. S. Department of Commerce
Washington 25, D. C.

LA-2811
UC-34, PHYSICS
TID-4500 (18th Ed.)

LOS ALAMOS SCIENTIFIC LABORATORY
OF THE UNIVERSITY OF CALIFORNIA LOS ALAMOS NEW MEXICO

REPORT WRITTEN: December 1962

REPORT DISTRIBUTED: February 18, 1963

BETA DECAYS AND DELAYED GAMMAS FROM FISSION FRAGMENTS

by

James Griffin

Contract W-7405-ENG. 36 with the U. S. Atomic Energy Commission

ABSTRACT

A theoretical study is made of the gross behavior of beta decays following nuclear fission in times from 10^{-2} to 10 seconds. First a simple model is formulated to describe the situation in terms of a few parameters. Then the most uncertain of these parameters are chosen to fit the observed rate of delayed gamma emission (assumed proportional to the beta-decay rate) for the $U^{235}(n,f)$ process. The description is extended to other isotopes by assuming that they differ only by small shifts of their initial fragment distributions away from that appropriate to neutron-induced fission of U^{235}. The result is a theoretical summary of the presently available data which can be used in predictive extrapolation of that data to situations not yet studied experimentally.

ACKNOWLEDGMENT

The author would like to express his gratitude to Mr. Kenneth Crandall, who programmed and carried out the calculations reported.

CONTENTS

CONTENTS
(Continued)

Page

FIGURES

I. GENERAL DESCRIPTION OF POST-FISSION DECAYS

In a short time following nuclear fission, several neutrons are emitted from the highly excited separating fragments. Then the remaining excitation energy is removed by the rapid emission of gamma radiation until the fragment reaches its ground state, or, in a few cases, an excited isomeric state whose decay is much slower than typical gamma decays. Most of this gamma radiation is emitted within 10^{-6} seconds after fission,[1] although gamma rays (presumably isomeric) continue to be emitted at an observable and steadily decaying rate for times as long as 10^{-3} seconds after fission.[2]

For the typical fragment, the time between 1 millisecond and 1 second after fission is a dull period of inactivity because, since it has emitted enough gamma radiation to reach its ground state, its next decay must be a beta decay, which requires a time of the order of seconds. During this period a few beta decays will, of course, occur, followed by gamma emission whenever the beta decay goes to an excited state of the daughter nucleus. For times short compared to 10^{-1} seconds, these decays are so few as to

leave the populations of the various fragments essentially unchanged. The observed average decay rate should therefore be constant during this interval, as should the rate of delayed gamma emission arising from beta decays to excited states. Thus, provided only that the intensity of long-lived prompt gammas has diminished so that it is small compared to this constant intensity of delayed gammas following beta decay, one ought to expect a plateau in the observed rate of gamma emission extending to times of the order of 10^{-1} seconds. Such a plateau has, in fact, been observed in the photon-induced fission of U^{238} with pulsed beams.[2]

For times greater than 1 second, enough beta decays occur to begin shifting the fragment population closer to the line of stability. This shift effects a decrease in the average beta-decay energy with a consequent decrease in the average rate of beta decay and of subsequent delayed gamma emission. Thus one expects the observed gamma rate to decrease again for times of the order of seconds, as observed.[1,2]

The time dependence expected from the above description is indicated qualitatively in Figure 1.

II. SIMPLIFIED MODEL FOR POST-FISSION BETA DECAY

Rather than attempt to consider the initial (after neutron emission) distribution of the fission fragments in its full detail and to trace the subsequent development of this distribution in time, we replace that distribution by a single beta-decay chain, $\bar{A}$, whose characteristics are

chosen to represent the average characteristics of the full distribution. We therefore assume for this chain a simple dependence of the nuclear masses on the displacement from the line of stability.

$$M(\bar{A},Z) = c_1(Z - Z_s)^2(\pm\Delta) \qquad (1)$$

The Δ is added when a nucleus is odd-odd (i.e., has odd proton and neutron numbers), subtracted when the nucleus is even-even, and omitted for odd-even or even-odd nuclei. The maximum energy of a beta decay from a given nucleus (A,Z) in the chain to the daughter nucleus $(\bar{A},Z - 1)$ is therefore taken to be

$$E_\beta^{max} = \left.\frac{\partial M(\bar{A},Z)}{\partial Z}\right|_{A=\text{constant}} = 2c_1(Z - Z_s) + \begin{cases} \pm 2\Delta \\ + 0 \end{cases} \qquad (2)$$

where $M(\bar{A},Z)$ describes a section through the nuclear mass surface chosen to reproduce the average properties of the fission fragments, and Z_s is the value of Z at the minimum of the parabola, Eq. (1); i.e., at the line of stability.

Thus our single idealized chain actually consists of two chains, one composed of odd-mass, and one of even-mass, nuclides. In the latter case, the addition and subtraction of the quantity 2Δ is made to alternate beta decays. These two possibilities are given equal weight in the calculation since there appears to be no strong preference for nuclear fission fragments to have either odd or even mass.[3]

Actually, in calculation, the even-mass chain is also divided into two parts so that decays whose energy is enhanced by $+2\Delta$ in one correspond to decays whose energy is diminished in the other. This is merely a device to avoid any possible systematic bias arising from an arbitrary choice of enhancement for one specific half of the decays. The constant c_1 in Eq. (2) is chosen to be the average of the corresponding constants in the semi-empirical mass formula in the regions of the heavy and light fragments.

The fragments are assumed initially to be distributed along this average chain with a probability described by a Gaussian function

$$P(z) = \frac{1}{\sqrt{\pi\delta}} \exp - \frac{(z - \bar{z})^2}{\delta} \qquad (3)$$

where $z = Z - Z_s$ is the displacement in charge from stability. This distribution involves two constants, δ and $\bar{z}$. The former is taken from measurements of the width of the distribution of charges of fission fragments about the most probable charge,[4] as is the Gaussian form of the distribution. The latter constant, $\bar{z}$, varies somewhat with the fissioning isotope, and such variations result in significant systematic differences among different isotopes. The specification of this constant will be discussed in more detail.

After the above specification of the initial situation, the various beta decays are allowed to proceed, and the time development of the population, $P(z)$, is calculated, together with the average beta-decay rate

at each time. During this process, a beta decay at point z diminishes the population P(z) and increases the population P(z - 1). To carry out this calculation it is, of course, necessary to assign a beta-decay rate to each element, z, of the fragment population. This rate is taken to be[5]

$$\lambda(z) = c_2 \overline{[w(z)]^5} \tag{4}$$

where

$$w(z) = \left[(\bar{E}_\beta)^2 - m^2c^4 \right]^{1/2} \tag{5}$$

is the beta end-point energy for decays at the point z on the chain. (Here m is the electron rest mass.) The averaging of $\overline{w^5}$ is made at ten points equally spaced within each unit interval. The constant c_2 is related to the average value of ft, proportional to the square of the beta-decay matrix element, for the beta decays in question.

In all these calculations, c_2 is required to have the same value for all the isotopes considered. This condition follows from the reasonable assumption that slight changes in the initial population have no effect on the average matrix elements of the many beta decays occurring. It plays the practical role of limiting the calculational freedom available in the process of fitting the observations.

The quantity $\bar{E}_\beta$ in Eq. (5) is not, of course, given by the maximum decay energy described by Eq. (2) because beta decays typically proceed to some excited state of the daughter nucleus. One has, therefore,

$$\bar{E}_\beta = E_\beta^{max} - E_\gamma \qquad (6)$$

where E_γ is the average gamma-ray energy associated with the type of beta decay in question. The specification of E_γ is discussed in some detail in the following section.

III. GAMMA RADIATION FOLLOWING BETA DECAY

The characteristics of gamma radiation expected following beta decay can be summarized in a general way by discussing the known characteristics of the spectra of even-even, odd mass, and odd-odd nuclei. According to the pairing model[6] of nuclei, even-even nuclei should exhibit a distinct scarcity of particle-type excited states for energies less than that required to "break a pair" of ground state nucleons (about one or two Mev). Odd mass nuclei, on the other hand, have already in the ground state one unpaired particle (or better, "quasi-particle"). Excited states can, in this case, be generated simply by placing this quasi-particle in various orbits. The resulting density of such excited states corresponds roughly to the expected density of single-particle states in a Fermi gas of nuclear density. Odd-odd nuclei have two quasi-particles in the ground state and thus exhibit an even greater density of excited particle states near the ground state than do odd mass nuclei. Such spectra are illustrated in Figure 2.

For beta decay one has, therefore, three general classes of transition: (e,e) → (o,o) and (o,o) → (e,e) for even mass chains, and (o,e) → (e,o) for odd mass chains. These are expected, on the average, to have maximum beta-decay energies changed by -2Δ, $+2\Delta$, and 0, respectively, from the decay energies characteristic of a smooth semi-empirical mass surface appropriate to odd mass nuclei. This feature has already been incorporated into Eq. (2).

However, it is also expected that the tendency of beta decay to go to excited states rather than the ground state of the daughter nucleus will differ among the three classes, so that the average beta decay energy will not follow precisely the behavior of the maximum beta decay energy.

In Figure 3 we portray schematically the three beta-decay classes and indicate the maximum-energy beta decays associated with each. Also indicated is the expected average beta decay, which differs from the maximum beta decay by the added requirement that the final state in the daughter be similar in character to the decaying ground state of the parent. For (o,e) → (e,o) transitions, both initial and final states involve one quasi-particle. In general, however, angular momentum selection rules will favor decay to some excited state assumed to lie above the ground state by an amount E_γ^o, on the average. For (e,e) → (o,o) transitions, the initial state has no excited quasi-particles, whereas the final states available involve two quasi-particles. In an odd-odd nucleus, however, these lie close to the ground state, and higher excited

states involve two or more quasi-particles. For simplicity, it is assumed that the preferred final state will lie above the ground state by the same energy, E_γ^o, used to characterize (o,e) decay. Finally, odd-odd parents with two quasi-particle ground states decay to even-even daughters whose lowest two quasi-particle states lie about 2Δ above the ground state. We assume again that decay will occur to a state which lies an energy E_γ^o above the lowest two-quasi-particle state. The resulting energies of gamma rays associated with each of the classes of decay are summarized in Table I.

From the even-odd mass differences based on semi-empirical mass studies,[7] we choose $\Delta = 0.90$ Mev. The value of E_γ^o is chosen in conjunction with the value of c_2 to optimize the description of $U^{235} + n$, for which both gamma[8] and beta-decay[9] rates have been measured. This choice is described in more detail below.

IV. CALCULATIONS

The time dependence of the beta-decaying population is computed by straightforward time steps from the initial population, Eq. (3) (approximated by eight discrete elements, $P_j^\tau(t)$, spaced at integral values of $z = z_o$), and from the decay rates, λ_j^τ, associated with each such element via Eq. (4). The index τ denotes the three portions of the chain corresponding to the discussion of Section II. Thus one computes $P_j^\tau(t + \Delta t)$

TABLE I

Assumed Characteristics of Various Types of Beta Decay

Type of Decay	$(o,e) \rightarrow (e,o)$	$(e,e) \rightarrow (o,o)$	$(o,o) \rightarrow (e,e)$
E_β^{max}	$(\partial M/\partial Z)_{A=const} = E_\beta^o$	$E_\beta^o - 2\Delta$	$E_\beta^o + 2\Delta$
Relative Weight	0.5	0.25	0.25
Gamma Energy*/Beta Decay	$E_\gamma^o = 1.03$ Mev	$E_\gamma^o = 1.03$ Mev	$E_\gamma^o + 2\Delta = 2.83$ Mev
$\bar{E}_\beta$	$E_\beta^o - E_\gamma^o$	$E_\beta^o - 2\Delta - E_\gamma^o$	$E_\beta^o - E_\gamma^o$

*E_γ^o is a parameter fixed by data on U^{235} as discussed in Section VI.

from $P_j(t)$ by the equation:

$$P_j^\tau(t + \Delta t) = P_j^\tau(t) \left[1 - D_j^\tau \Delta t\right] + P_{j+1}^\tau(t) \cdot D_{j+1}^\tau \cdot \Delta t \qquad (7)$$

where

$$D_j^\tau = \lambda_j^\tau \quad \text{when} \quad \lambda_j \Delta t \leq 1 \qquad (8)$$

$$= 1/\Delta t \quad \text{when} \quad \lambda_j \Delta t > 1$$

The magnitude of the time step, Δt, at time t is chosen to be a fraction $1/q$ times the slowest decay period associated at time t with 1 percent or more of the population. Values $q \geq 3$ have been used in all the calculations reported here.

Having determined the time dependence of the population, one computes the time dependent beta-decay rate directly for each time

$$\bar{\lambda}(t) = \sum_{j\tau\sigma} \lambda_j^{\tau\sigma} P_j^{\tau\sigma}(t) g^\tau \qquad (9)$$

where the weights g^τ for the three chains have the value 1/2, 1/4, 1/4 as discussed in Section II, and the index σ corresponds to the three types of beta decay [(o,e) → (e,o); (e,e) → (o,o); (o,o) → (e,e)]. The corresponding rate of post-beta gamma emission is similarly evaluated

$$\dot{E}_\gamma(t) = \sum_{j\tau\sigma} E_\gamma^\sigma \lambda_j^{\tau\sigma} P_j^{\tau\sigma}(t) g^\tau \qquad (10)$$

The values of E_γ^σ are given in Table I. Finally, the rate of emission of energy from the beta-decay process (comprising the kinetic energy of the electron and of the emitted antineutrino) is calculated by

$$\dot{E}_\beta(t) = \sum_{j\sigma\tau} w_j^\sigma \lambda_j^{\tau\sigma} P_j^{\tau\sigma}(t) g^\tau \qquad (11)$$

where w_j^σ is given by Eq. (5), evaluated at $z = z_j$ with $\bar{E}_\beta$ as given for each type of decay, σ, in Table I.

V. APPROXIMATIONS AND LIMITATIONS

Various approximations have been made in the present analysis, besides the overall assumption that the complexity of the system of decaying fission fragments is sufficient to justify such an averaged few-parameter description as that employed here.

In particular, Eq. (4) is appropriate only when $w(z) > 5\ mc^2$. This means that our description can be accurate only when the largest fraction of the beta decays involves at least this much energy; i.e., only for times less than $1/c_2(5)^5 \approx 2$ sec. Actually, the results suggest that this statement is somewhat too stringent: serious discrepancies between calculation and experiment set in only at times about 10 seconds after fission.

Another aspect of the present calculations which limits the length of time over which the description is accurate, even in the absence of the above approximation, is the excessive granularity of the structure of the decaying groups by the time the population has shifted to within one or two decays of the line of stability. At this stage, the present calculation describes subsequent decay in terms of one or two groups with precisely specified decay times rather than of the broad distribution of groups which would more resemble the actual situation of the twenty to thirty fission fragments being described. This deficiency is, of course, purely a calculational one and could easily be obviated if one were especially interested in describing the behavior at later times than these considered here.

Still a third inaccuracy which becomes more serious at long times is the rigid prescription that some specified fixed energy is to be subtracted from each maximum beta-decay energy to account for de-excitation gamma radiation. In the calculation, this leads, of course, to the assignment of an infinite beta lifetime to certain decays whose maximum beta energy is low, although physically these decays will still occur, but with an extended lifetime and associated with less than the average gamma energy. This oversimplification obviously is more serious for decays which are initially assigned a low maximum beta-decay energy; i.e., to decays close to stability, which dominate the situation only at later times than those emphasized here.

Indeed, it must be mentioned that, even for short times, the particular distribution of gamma energy among the three classes of beta decay which has been adopted here is based primarily on theoretical expectation. It would seem likely that agreement between calculation and experiment just as good as that obtained here could be based on the other assumptions, e.g., that a fixed constant gamma energy is emitted following each beta decay or that the gamma energy emitted is a fixed fraction of the maximum possible decay energy. The present assumption seems the most consistent with recent developments in the theory of nuclear structure, and is therefore preferred, with the restriction that no freedom is allowed in adjusting the corresponding parameters beyond the specification of the single quantity, E_γ^o.

VI. SPECIFICATION OF PARAMETERS

The important physical parameters which specify given calculations based on the present model are the following:

(1) $\bar{z}$ - the average displacement of the initial distribution from stability;

(2) E_γ^o - the average gamma energy in excess of the assumed minimum for each type of beta decay;

(3) c_2 - the characteristic beta-decay rate;

(4) c_1 - the coefficient of the mass parabola;

(5) δ - the width of the initial distribution;

(6) Δ - the even-odd mass difference.

The last three parameters in the present treatment are chosen once and for all at the outset, and no variation is allowed. Thus δ is taken equal to 1.0 from the work of Reference 4, and $\Delta = 0.90$ Mev and $c_1 = 1.61\ mc^2$ are chosen as the average over the mass regions of the heavy and light fragments of the empirical value given by Reference 7.

The second and third parameters are chosen to optimize the fit to the U^{235} data, a procedure discussed in detail below. Once so fixed, these parameters are held fixed for calculations directed at other nuclides.

1. Specification of Parameters E_γ^o and c_2

As noted above, the parameters E_γ^o and c_2 are chosen to optimize the agreement between the calculation and the experimental data for U^{235}. This optimization will now be discussed in some detail.

The experimental data are of two types:

(a) the rate of emission of gamma energy, $\dot{E}_\gamma(t)$, after beta decay measured by Engle et al.[8]

(b) the rate of beta decay, $\bar{\lambda}(t)$, measured by Armbruster[9] (called $\beta(t)$ in that reference).

Actually, Engle's data were interpolated to the convenient times listed (together with the interpolated values) in Table II. The estimated error given by these authors is $\pm$ 15%, which is also listed as $\sigma(\dot{E}_\gamma)$.

TABLE II

U^{235} Data Used in Fitting Parameters*

t (Sec)	$\dot{E}_\gamma \pm 15\%$ $(\frac{\text{Mev}}{\text{Sec}})$	$\bar{\lambda}$ $(\frac{\text{Decays}}{\text{Sec}})$	$\dot{E}_\gamma/\bar{\lambda} \pm 15\%$ $(\frac{\text{Mev}}{\text{Decay}})$
0.3	0.58 ± 0.087	0.37	1.57 ± 0.24
1.0	0.38 ± 0.057	0.32	1.19 ± 0.18
3.0	0.21 ± 0.032	0.18	1.17 ± 0.18
10.0	0.079 ± 0.012	0.068	1.16 ± 0.17

*This table lists, for various times, t, the experimental values of $\dot{E}_\gamma$ (interpolated from Ref. 8) and $\bar{\lambda}$ (taken from Fig. 9 of Ref. 9) together with their ratio $\dot{E}_\gamma/\bar{\lambda}$. The parameters were chosen to give the best fit to $\dot{E}_\gamma$ and $\dot{E}_\gamma/\bar{\lambda}$ assuming the error in each due solely to the ± 15% error quoted for $\dot{E}_\gamma$.

For corresponding times, the value of $\bar{\lambda}(t)$ was taken from the smooth curve (Fig. 10) of Reference 9. These values are also listed in Table II.

Also listed in Table II is the ratio, $\dot{E}_\gamma/\bar{\lambda}$, together with the error implied by the ± 15% error in $\dot{E}_\gamma$. This ratio and the values $\dot{E}_\gamma$ were the data used to obtain the best values of the parameters c_2 and E_γ°. If one had good estimates of the errors associated with the measured values of $\bar{\lambda}(t)$, it would probably be better to optimize the fit to $\dot{E}_\gamma(t)$ and $\bar{\lambda}(t)$. Since such information is not available, and since, indeed, a rather careful analysis would be required to obtain it (because $\bar{\lambda}(t)$ is the derivative of a cumulative, and thus highly correlated, sequence of

measurements), we have chosen the present procedure. It should be valid if only the error in $\bar{\lambda}(t)$ is much less than ± 15%.

For several values of E_γ^o, the value of

$$\chi^2 = \sum_{j=1}^{8} \frac{(E_j - T_j)^2}{\sigma_j^2} \tag{12}$$

was computed as a function of c_2. E_j and σ_j represent empirical quantities listed in columns 2 and 4 of Table II, and T_j is the corresponding calculated quantity. The resulting curves for E_γ^o = 1.00, 1.02, and 1.04 Mev are plotted in Figure 4. From each such curve, the minimal value of χ^2 together with the value of c_2 at that minimum was plotted (also in Fig. 4) indicating an absolute minimum when $c_2 = 3.25 \times 10^{-6}$/sec. This value implies log ft ≈ 4.5 for the average beta decay, according to the calculations of Feinberg and Trigg.[10] The corresponding value of E_γ^o was determined by plotting the values of E_γ^o to the corresponding minimal value of c_2. The result was E_γ^o = 1.03 Mev.

2. Specification of Average Chain Length, $\bar{z}$

Finally, one has to specify the value of $\bar{z}$ for each isotope considered. We consider the neutron-induced fission of a nucleus (Z,A) with the emission of ν prompt neutrons. Then the two fragments L and H of the initial beta-decay population have

$$A_L + A_H = A + 1 - \nu \tag{13}$$

$$Z_L + Z_H = Z \tag{14}$$

For given A_L and A_H, the line of stability determines Z_L^s and Z_H^s, and the total displacement of both fragments from stability is equal to

$$Z_L^s + Z_H^s - Z \tag{15}$$

The quantity $\bar{z}$ should be taken to be the average of this quantity over the various mass divisions consistent with Eq. (17) weighted with the observed mass yield curve. For U^{235} + n (with $\nu = 2.5$) we have computed this average with the simplifying assumption that the mass yield is constant for fragment pairs from (Z,A) equal to (90,233.5) to (100,233.5). (A chain with half-integral mass is taken as the average of the adjacent chains.) In this way one obtains a total average displacement from stability of 7.08, which implies an average $\bar{z} = 3.54$ for each fragment.

To determine $\bar{z}$ for U^{235} in a Godiva spectrum (where $\nu = 2.58$) and for other nuclides, one can use a perturbative approach based on the assumption that $\bar{z}$ changes linearly for small modifications of A and Z.

In particular, consider the addition of p mass units, q of which are protons. Then

$$\bar{z}(A + p, Z + q) \approx \bar{z}(A,Z) + p\left[\frac{\overline{\partial z}}{\partial A}\right]_{Z=\text{const}} + q\left[\frac{\overline{\partial z}}{\partial z}\right]_{A=\text{const}} \tag{16}$$

where the derivatives indicated are averages over the fission mass

distribution. It is clear immediately that

$$\left.\frac{\partial \bar{z}}{\partial z}\right|_{A=\text{const}} = -0.50$$

that is, each and every total displacement, Eq. (15), is decreased by one unit for each unit increase in Z; the average displacement for each fragment is correspondingly decreased by one-half unit.

To estimate $\left[\frac{\partial \bar{z}}{\partial A}\right]_{Z=\text{const}}$ we have carried out the same averaging process for U-233 and U-237 (with $\nu = 2.5$ here also) as was described above for U^{235}. The estimates gave the results

$$\left[\frac{\partial \bar{z}}{\partial A}\right]_Z = \begin{cases} 0.20 & \text{for addition of 2 neutrons} \\ 0.24 & \text{for subtraction of 2 neutrons} \end{cases} \qquad (17)$$

We have therefore assumed $\left[\frac{\partial \bar{z}}{\partial A}\right]_Z = 0.22$ and computed $\bar{z}$ from the formula

$$\bar{z}(A,Z,\nu) = 3.54 + 0.22[A - 235 - \nu_N + 2.5] - 0.5[Z - 92] \qquad (18)$$

The resulting values of $\bar{z}$ for the various nuclides studied by Engle[8] are given in Table III.

3. Exclusion of Data for Later Times

We note that the fit to the short times ($t \leq 10$ seconds) actually considered is a much better fit than could have been obtained for all times up to 100 seconds. This circumstance is connected with the dips

TABLE III

Average Displacements, $\bar{z}$*

Target	E_n	ν	$\bar{z}$
U^{235}	G(1.47)	2.58	3.52
	2.00	2.80	3.47
U^{233}	G(1.47)	2.70**	3.05
U^{238}	G(1.47)	2.82	4.12
Th^{232}	1.60 Mev	2.08***	3.97
Pu^{239}	G(1.47)	3.06	3.29
	2.10	3.12	--

*This table presents the values of $\bar{z}$ used in the calculations, together with ν-values used to obtain them from the U-235 value via Eq. (19). The second column indicates the neutron energy, or a G in the case of a measurement in the reactor Godiva[11] with the mean energy of the Godiva spectrum in parentheses.

**This value of ν is obtained by adding to the value measured in the reactor Topsy the difference between the Godiva and Topsy measurements for U-235.

***This value of ν is obtained by extrapolating via Eq. (19) from data[11] at 3.5 Mev to the indicated (fission threshold) neutron energy.

in both $\bar{\lambda}$ and $\dot{E}_\gamma$ which the calculations exhibit for times between 10 and 100 seconds (Figs. 5 and 6). It can be traced to the excessive granularity of the eight discrete groups used in the present numerical calculations when sufficient time has passed for large fractions of the decaying population to have moved within about one unit of the line of stability. This is a calculational problem which could be solved by assuming a finer mesh of points, rather than a matter involving the physical processes described. Since our greatest interest here is in the short time behavior, we have chosen simply to omit from the determination of the best parameters comparison with calculated values which exhibit this malady (i.e., all $t > 10$ seconds).

VII. EXTRAPOLATIONS

In the present model, only the parameter $\bar{z}$ distinguishes among various targets and various excitation energies. We have therefore calculated $\dot{E}_\gamma$ $(t = 0)$ for several values of $\bar{z}$ and summarized the results in Figure 7. By means of this figure, Eq. (18), and the assumption that for a given nucleus

$$\nu(E_n') = \nu(E_n) + (E_n' - E_n)/7 \text{ (Mev)} \qquad (19)$$

(which appears to be quite a good approximation in cases measured so far)[11]

one can make an estimate of the early post-beta gamma radiation rate as a function of the energy of the neutron inducing fission if only one knows the value of $\bar{\nu}$ for the isotope at some neutron energy.

Moreover, even this last requirement can be relaxed by invoking the assumption that $\bar{\nu}$ is independent of neutron number for a given isotope at a given neutron energy. Although this assumption is much more difficult to assess theoretically than that concerning the increase of $\bar{\nu}$ with excitation energy,[12] it, too, appears to be a good approximation in those cases for which data is currently available.[11] Moreover, it is not unreasonable a priori to suppose that $\bar{\nu}$ is affected but little by the addition of neutrons, since the relevant division of energy at the scission point of nuclear fission appears to be dominated by Coulomb effects in which neutrons play no role.[13]

Of course each successive replacement of measured information by reasonable assumption leads to greater uncertainty in the final result. Nonetheless, it might be expected that reasonably good semi-quantitative estimates can be obtained in this way for relevant nuclei beyond the reach of laboratory study. We have therefore summarized in Table IV the the values of $\bar{z}$ implied by these assumptions for a variety of nuclei absorbing neutrons of 2 Mev and 14 Mev together with the corresponding post-beta gamma radiation rates at t = 0 implied by Figure 7.

TABLE IV

Extrapolated Estimates

Target Nuclide	E_n = 2 Mev $\bar{z}$	E_n = 2 Mev $\dot{E}_\gamma^o$ (Mev/Fiss.-Sec)	E_n = 14 Mev $\bar{z}$	E_n = 14 Mev $\dot{E}_\gamma(t=0)$	Godiva $\bar{z}$	Godiva $\dot{E}_\gamma(t=0)$
U^{233}	3.03	0.402	2.65	0.212	3.05	0.415
U^{234}	3.25	0.569	2.87	0.309	--	--
U^{235}	3.47*	0.795	3.09	0.442	3.52	0.856
U^{236}	3.69	1.090	3.31	0.624	--	--
U^{237}	3.91	1.465	3.53	0.871	--	--
U^{238}	4.13	1.941	3.75	1.184	4.12	1.917
U^{239}	4.35	2.549	3.97	1.584	--	--
U^{240}	4.57	3.317	4.19	2.092	--	--
Pu^{239}	3.29*	0.605	2.91	0.330	3.29	0.605
Pu^{240}	3.51	0.843	3.13	0.471	--	--
Pu^{241}	3.73	1.152	3.35	0.663	--	--
Pu^{242}	3.95	1.544	3.57	0.920	--	--
Pu^{243}	4.17	2.041	3.79	1.250	--	--
Th^{232}	--	--	--	--	3.97	1.584

*Values obtained from Table III (for specific neutron energies) corrected (for Pu-239) via Eq. (19).

VIII. RESULTS AND CONCLUSIONS

The results of the calculations are presented graphically in Figures 5, 6, and 8 through 15. For each of the nuclides included in the study of Engle and Fisher,[8] there appear calculated plots of $\dot{E}_\gamma$ vs. t, together with the experimental results of that study for comparison with the calculations. Finally, the calculated values of $\lambda(t)$ are plotted for these same nuclides, although no relevant data is currently available for comparison, except in the case of U^{235}.

These figures indicate that the present model is capable of describing the differences in post-beta gamma radiation rates observed for the different nuclides studied in Reference 8. The results also conform to the measurements of Reference 9 and the qualitative description of Section I, although it is now obvious that the normalization of U^{238} (γ,f) results to late time measurements[2] of U^{235} (n,f) is not a valid procedure.

The success of the model in describing the several measurements in terms of one independently estimable parameter encourages its extrapolation to other situations on which information is desired, but not yet available experimentally. For this reason we have made the extrapolations summarized in Table III, and provided Figure 7 to facilitate the estimates which other researchers might require.

It would be especially interesting to obtain experimental beta-decay rates for comparison with the calculated values of $\bar{\lambda}(t)$ for nuclides

other than U^{235}. Such data might allow refinement of the present parametrization of the model. It could also help to specify more closely the actual relationship between beta decay and subsequent gamma emission, which was taken in these calculations as an a priori theoretical assumption because of the lack of cogent experimental evidence.

Finally, it should be noted that results obtained from Eq. (6), together with the theoretical estimates by Perkins and King[14] of the division of energy between the electron and the anti-neutrino in beta decay, can be used to obtain theoretical results for the rate of energy released by electrons from beta decay for various situations, providing still another element for comparison, and still another basis for the resolution of the question of the relationship between beta decay and subsequent gamma emission.

IX. DISCUSSION OF ILLUSTRATIONS

Fig. 1. The qualitative time dependence of post-fission gamma radiation is indicated by three regions: in region a, the slow prompt gamma intensity (presumably from isomeric transitions) diminishes steadily with time until, at a', it becomes small compared with the gamma radiation following beta decay; this post-beta radiation intensity remains approximately constant, b, until a time comparable with a typical beta-decay half life; then it

decreases, c, as fast beta decays are replaced by slower ones as the population shifts towards the line of stability.

Fig. 2. This figure exhibits for the three types of nuclei the qualitative differences in the densities of levels near the ground state. The "gap," 2Δ, in even-even nuclei is about one or two Mev.

Fig. 3. This figure illustrates the discussion in the text, on the basis of which more gamma-ray energy is assumed to follow the decay of odd-odd nuclei than of even-even or odd mass nuclei.

Fig. 4. The upper portion of the figure shows curves of computed χ^2 for various fixed values of E_γ^o as a function of c_2. By constructing a smooth curve through the minima of these curves, the absolute minimum was located at the c_2 value shown. The lower portion shows the values of E_γ^o vs. c_2 at the minima of fixed E_γ^o curves. It was used to estimate the value of E_γ^o corresponding to the absolute minimum of the χ^2 family.

Fig. 5. The calculated rate of gamma emission (curve) is compared with the data of Engle and Fisher.[8] The parameters were chosen to optimize the fit to these data and those of Figure 6 as discussed in the text.

Fig. 6. The beta-decay rate calculated with the optimal values of E_γ^o and c_2 is shown (curve through points) together with points taken from the experimental curve of Armbruster et al.[9] (open circles). Values taken from the latter curve were used to choose E_γ^o and c_2. (See Table II.)

Fig. 7. This curve shows the relationship between the rate of gamma emission (following beta decay) and the average displacement, $\bar{z}$, of the fission fragments from the line of stability for the optimal values of c_2 and E_γ^o. It can be used to estimate such rates for times $10^{-3} < t < 10^{-2}$ seconds if some estimate of $\bar{z}$ is available for the fissioning nuclide.

Figs. 8 through 15. The calculated gamma rates (even-numbered Figures) and beta decay rates are exhibited. The former are compared with measurements of Engle and Fisher,[8] shown as points with those authors' estimated errors.

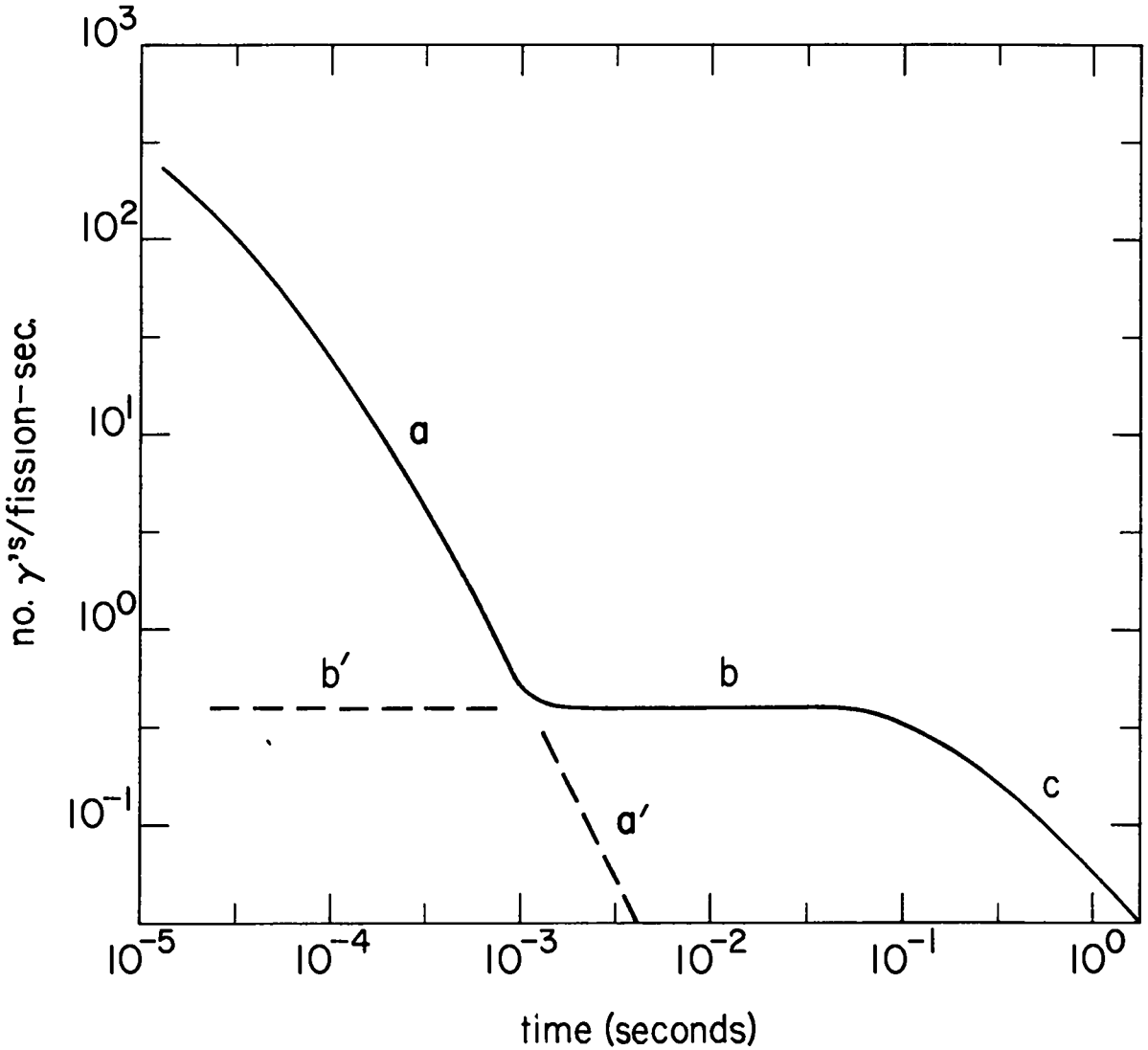

Fig. 1. Qualitative Time Dependence of Post-Fission Gamma Rate

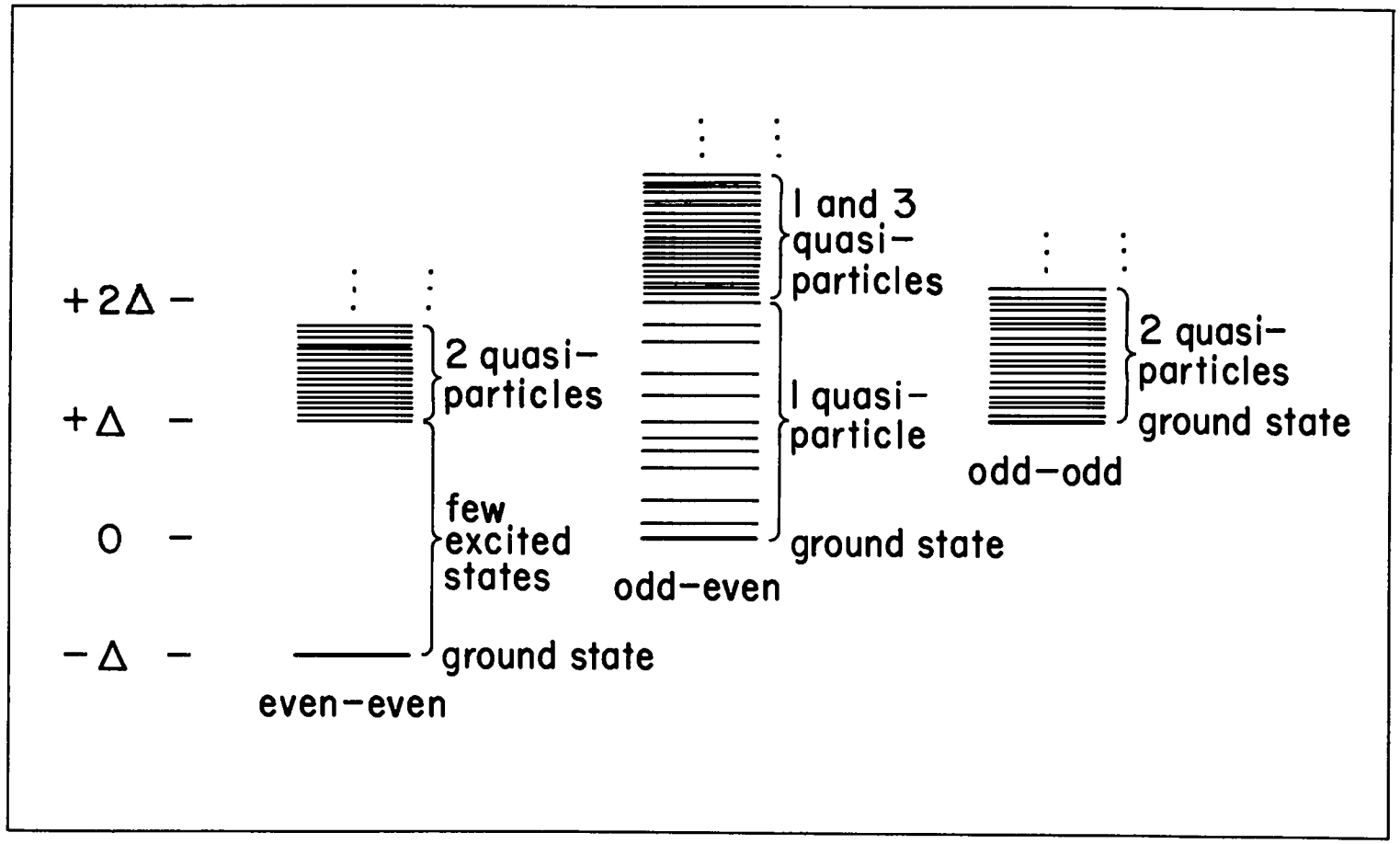

Fig. 2. Comparison of the Low-Energy Spectra of Even-Even, Odd Mass, and Odd-Odd Nuclei

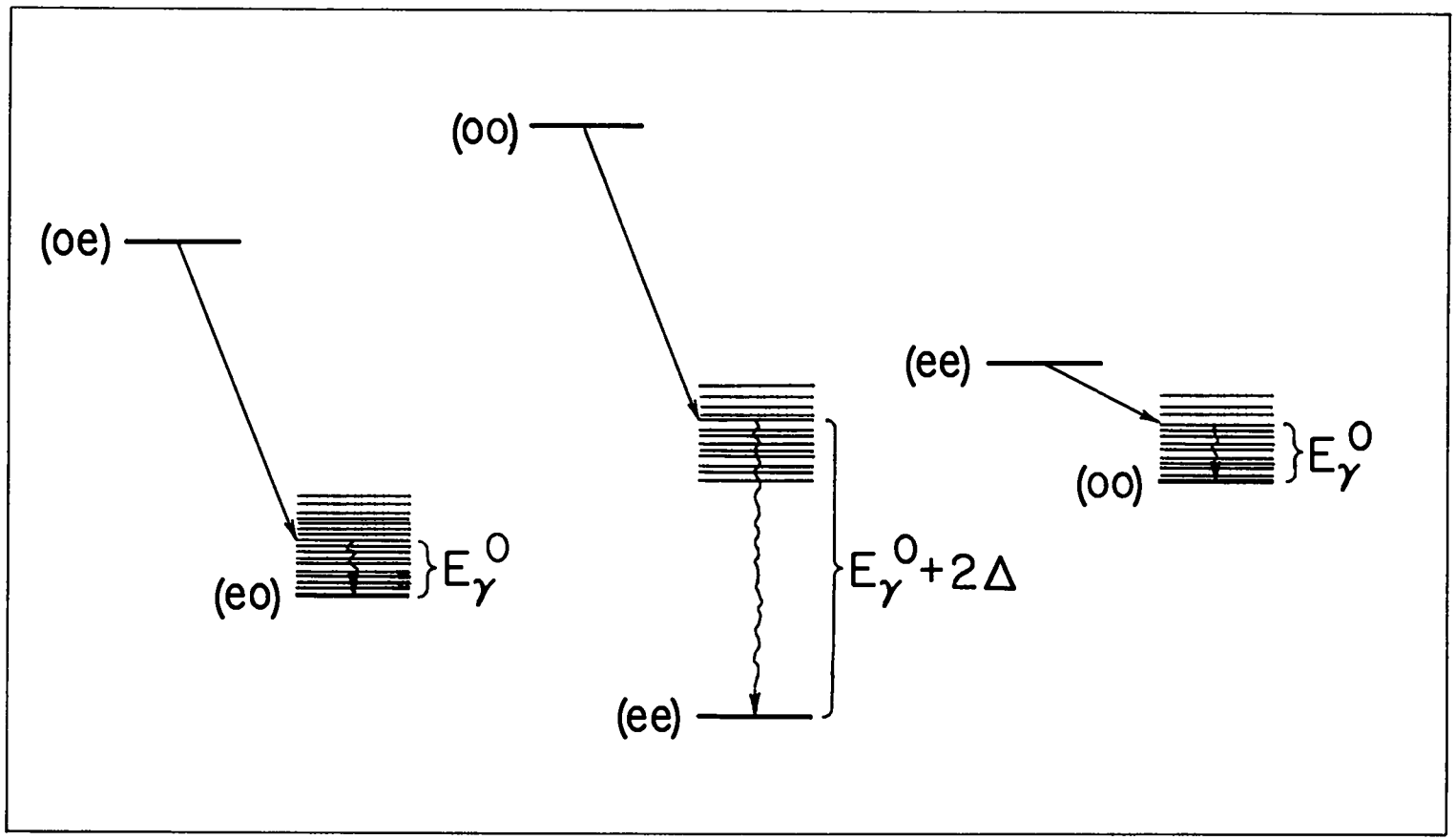

Fig. 3. The Average Gamma Energy Expected to Follow the Three Types of Beta Decay

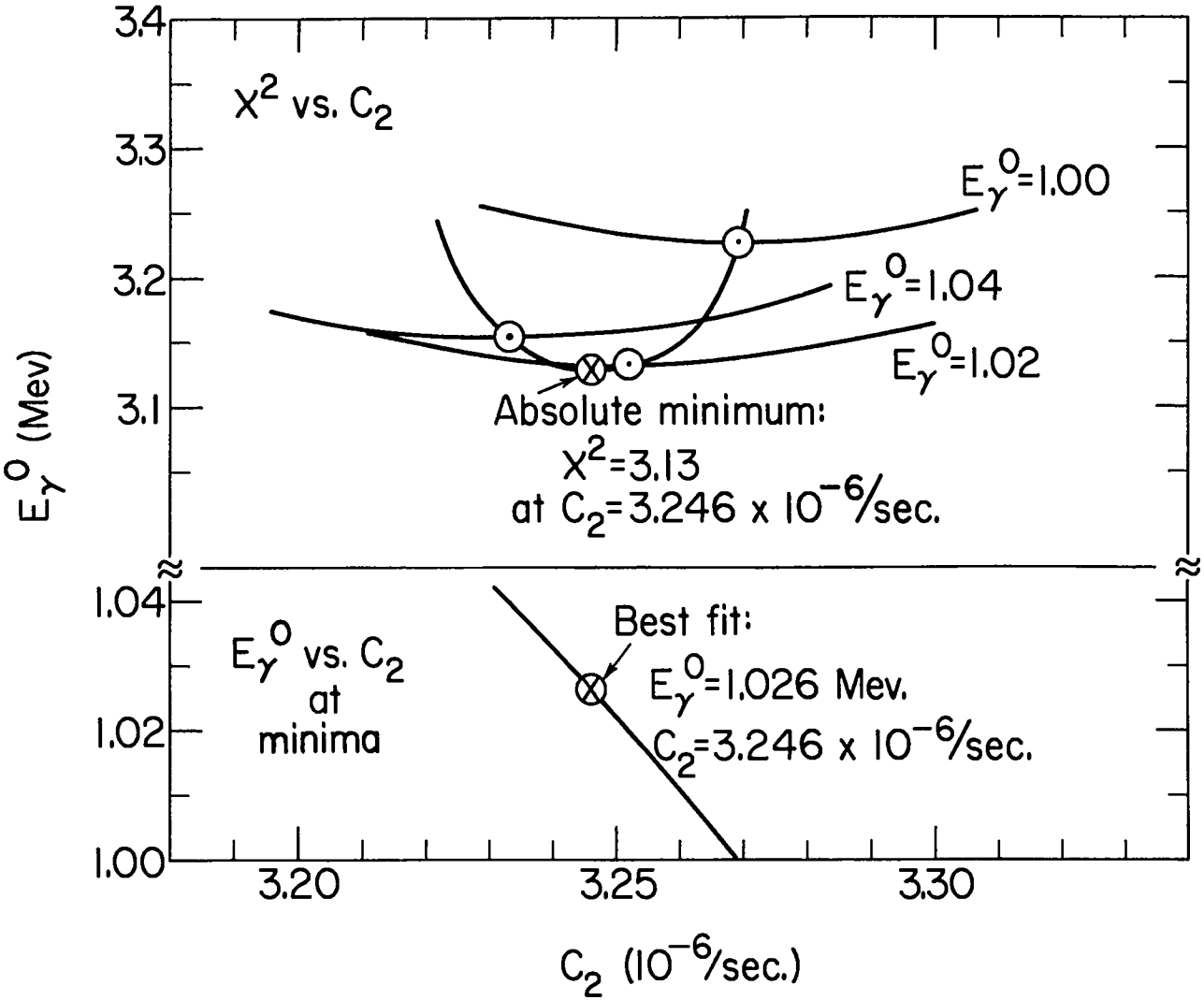

Fig. 4. Minimization of X^2 by Variation of E_γ^o and c_2

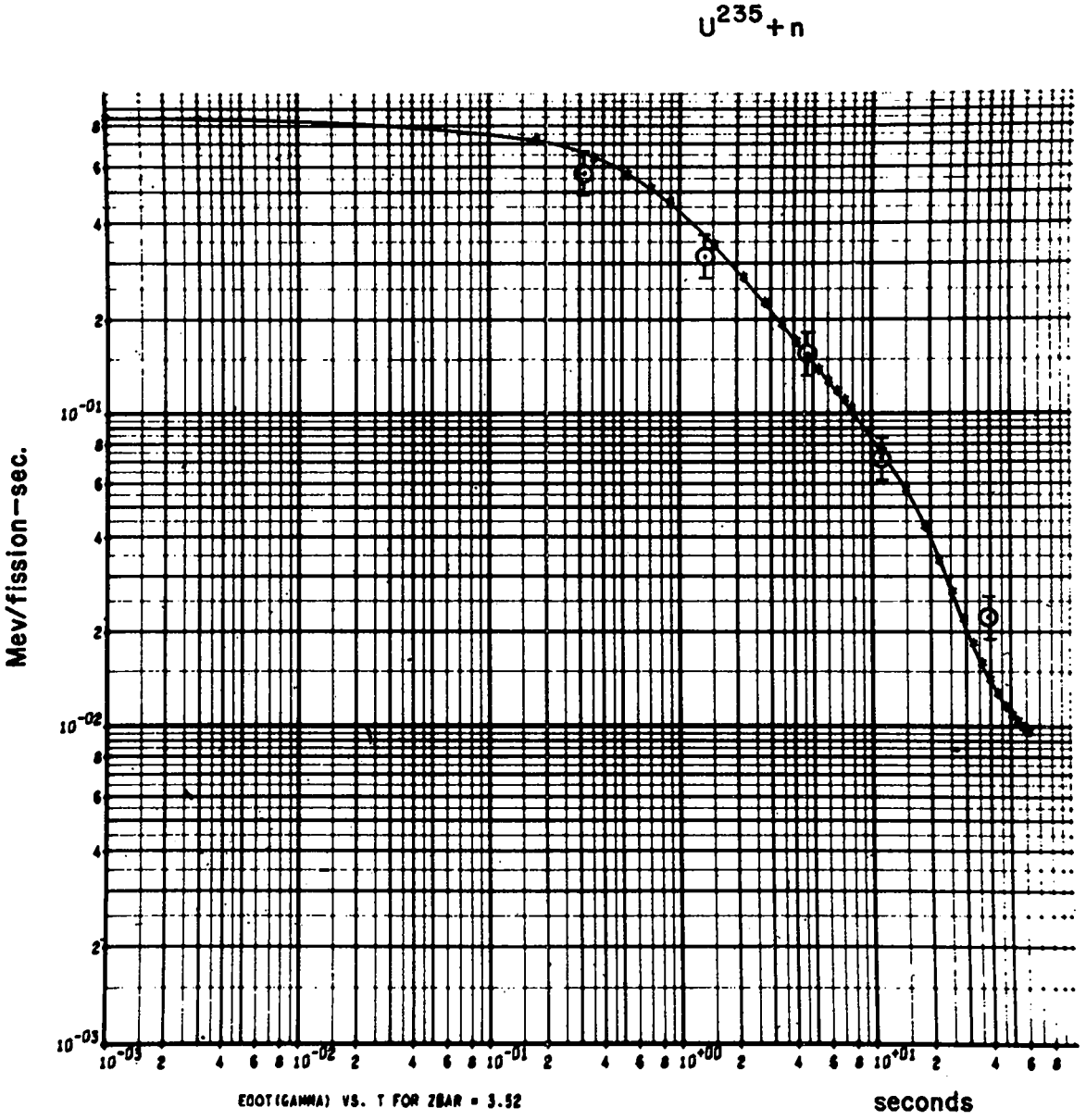

Fig. 5. Calculated and Observed Gamma Rates for U^{235}

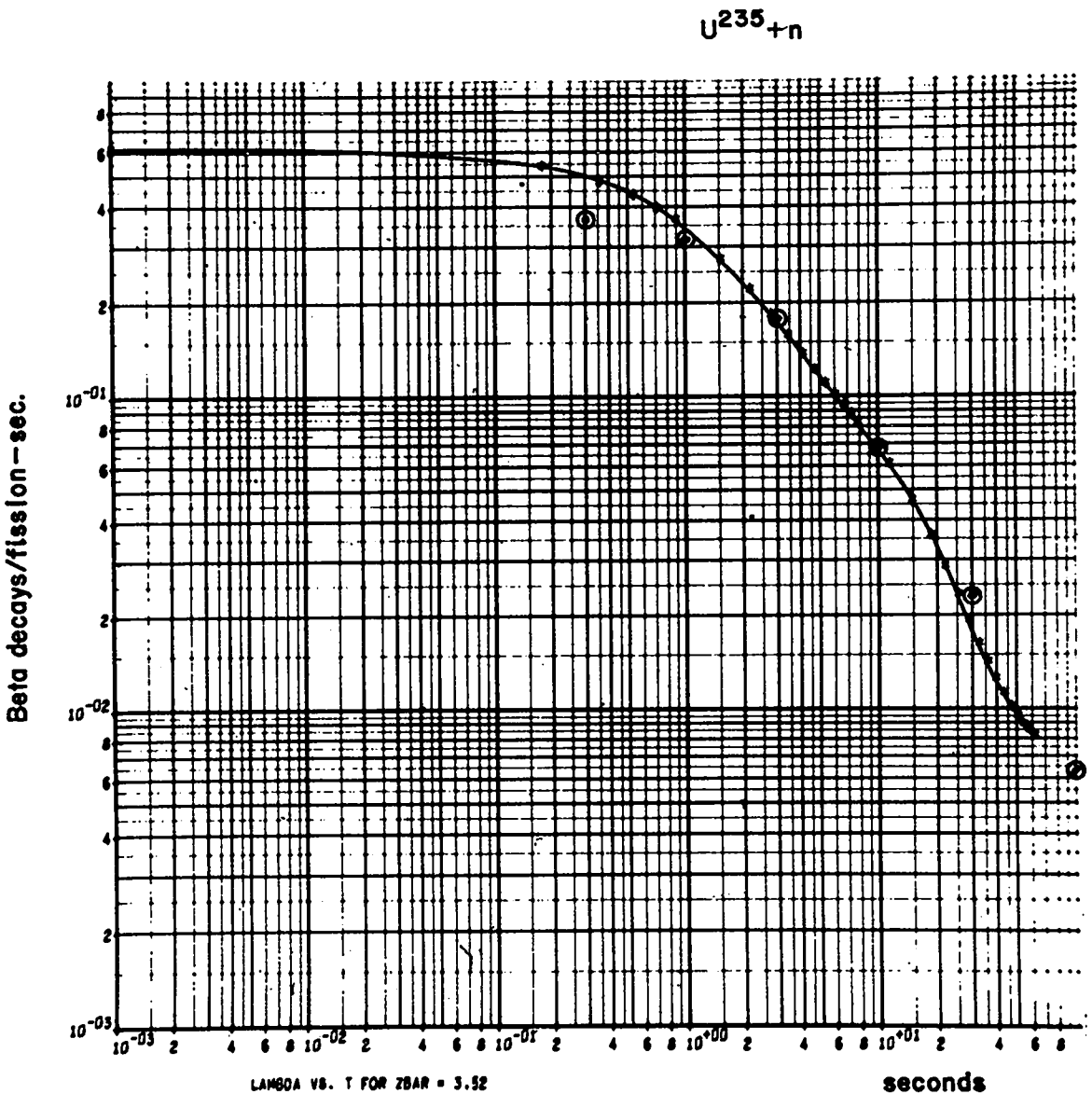

Fig. 6. Calculated and Observed Beta-Decay Rates for U^{235}

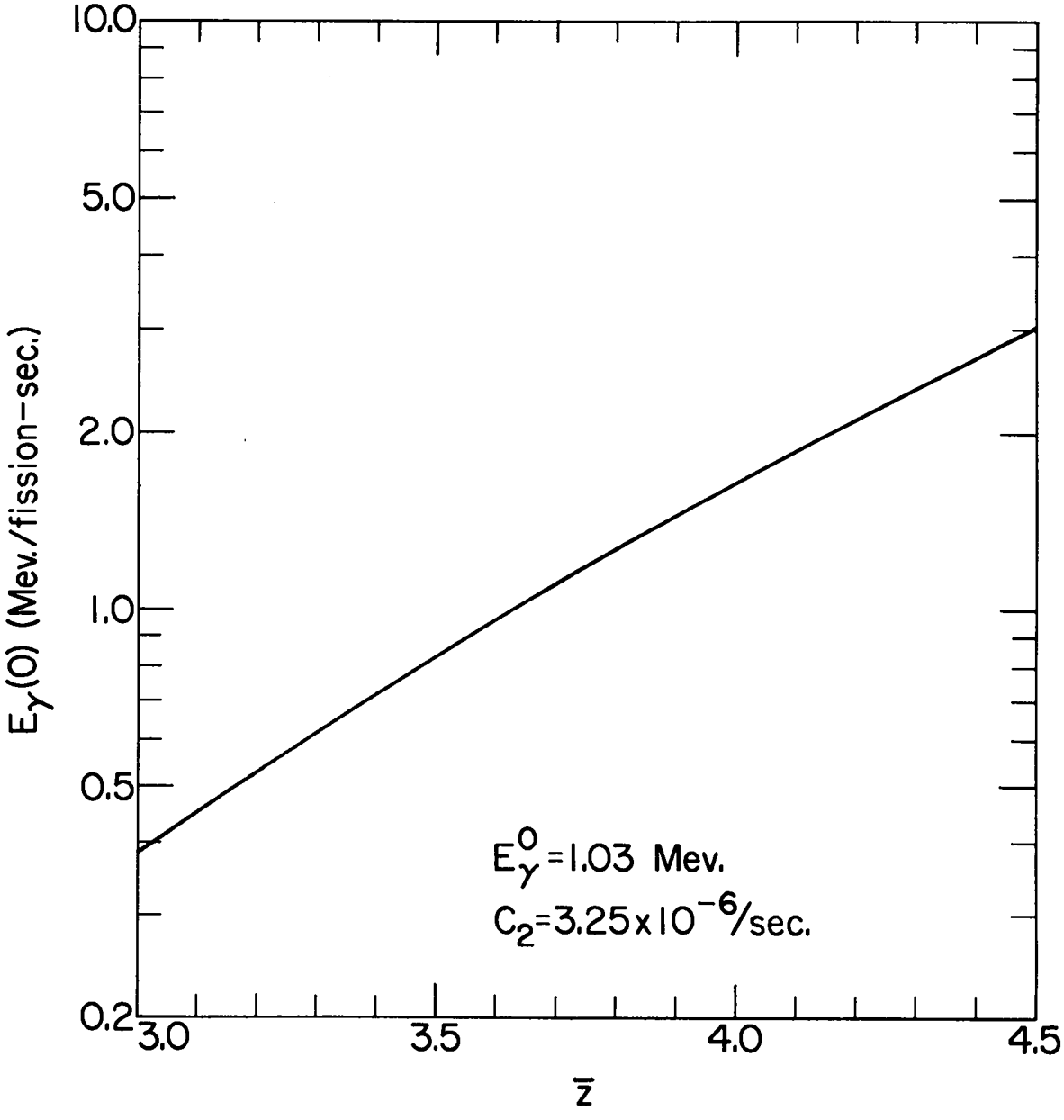

Fig. 7. Initial Gamma Rate vs. Average Displacement from Stability

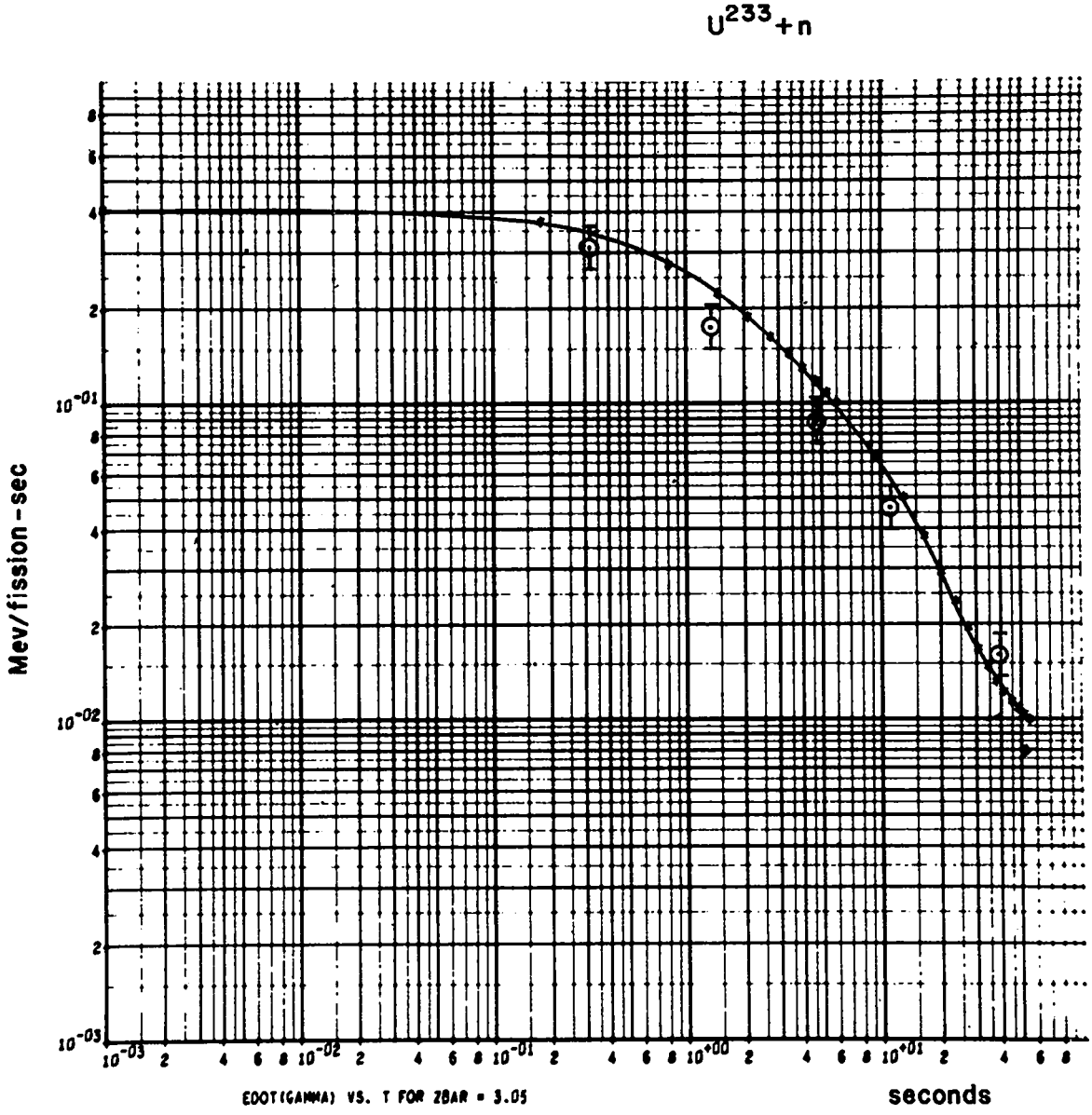

Fig. 8. Gamma Rate for U^{233} + n vs. Time

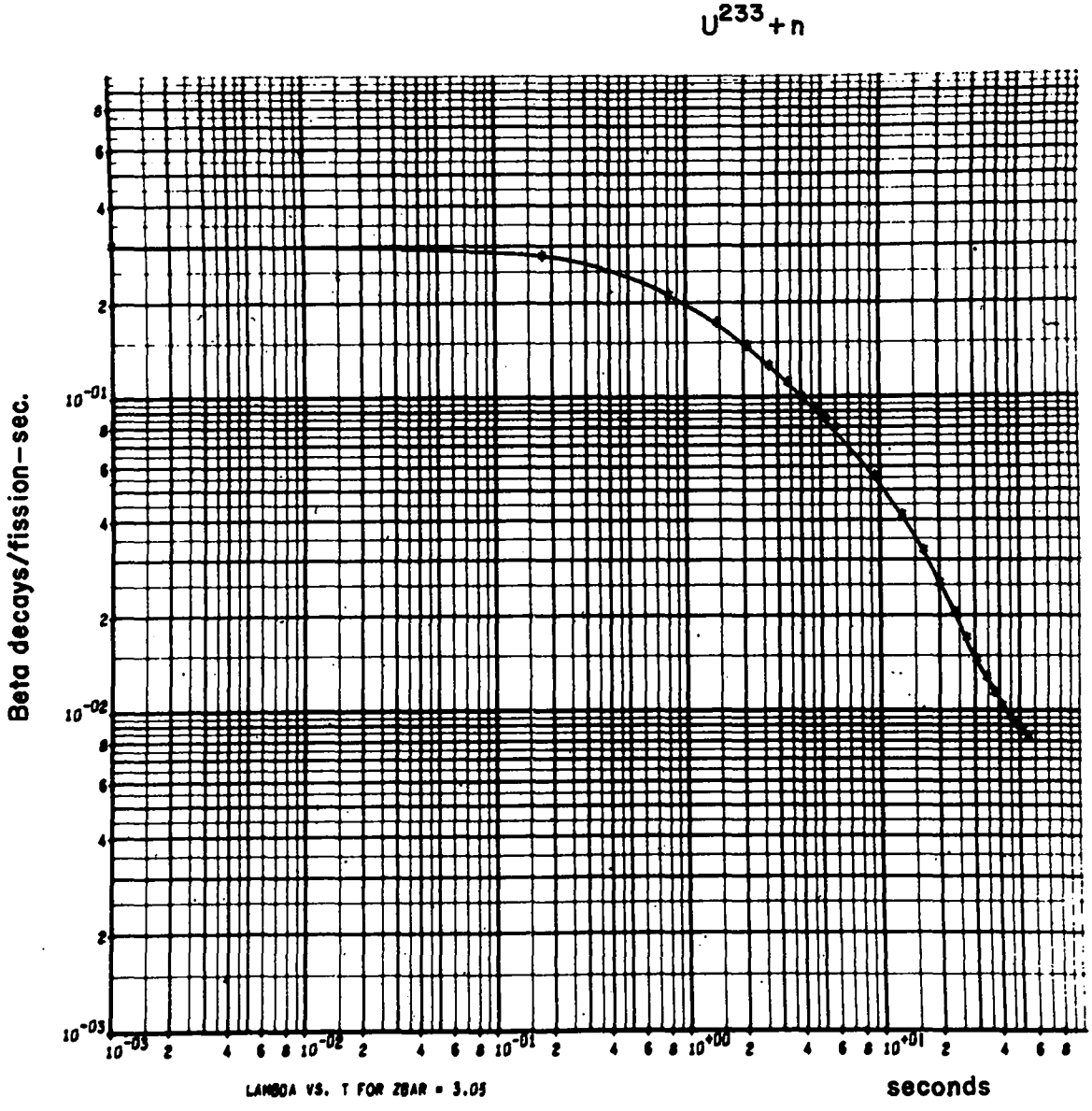

Fig. 9. Beta-Decay Rate for U^{233} + n vs. Time

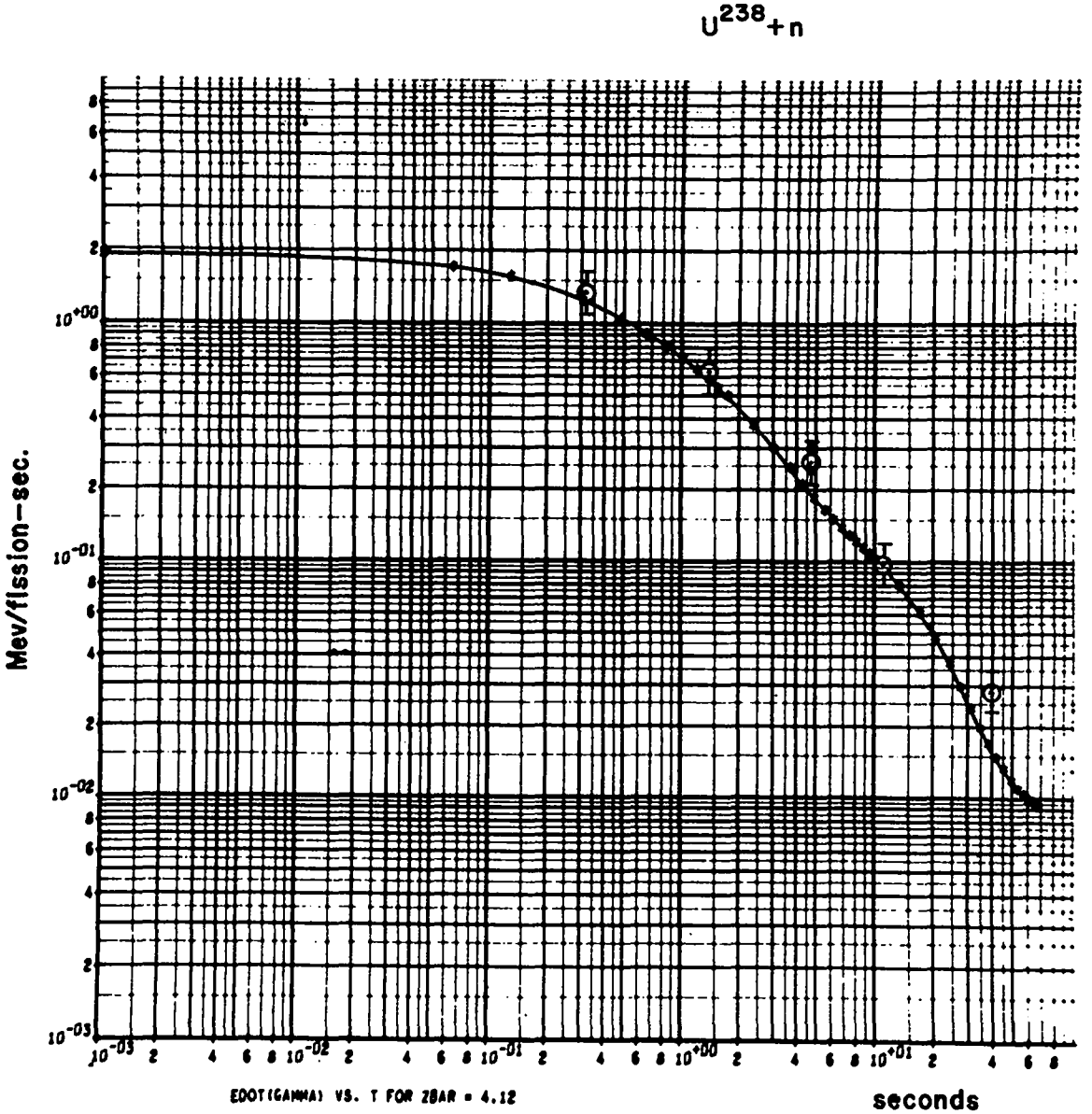

Fig. 10. Gamma Rate for U^{238} + n vs. Time

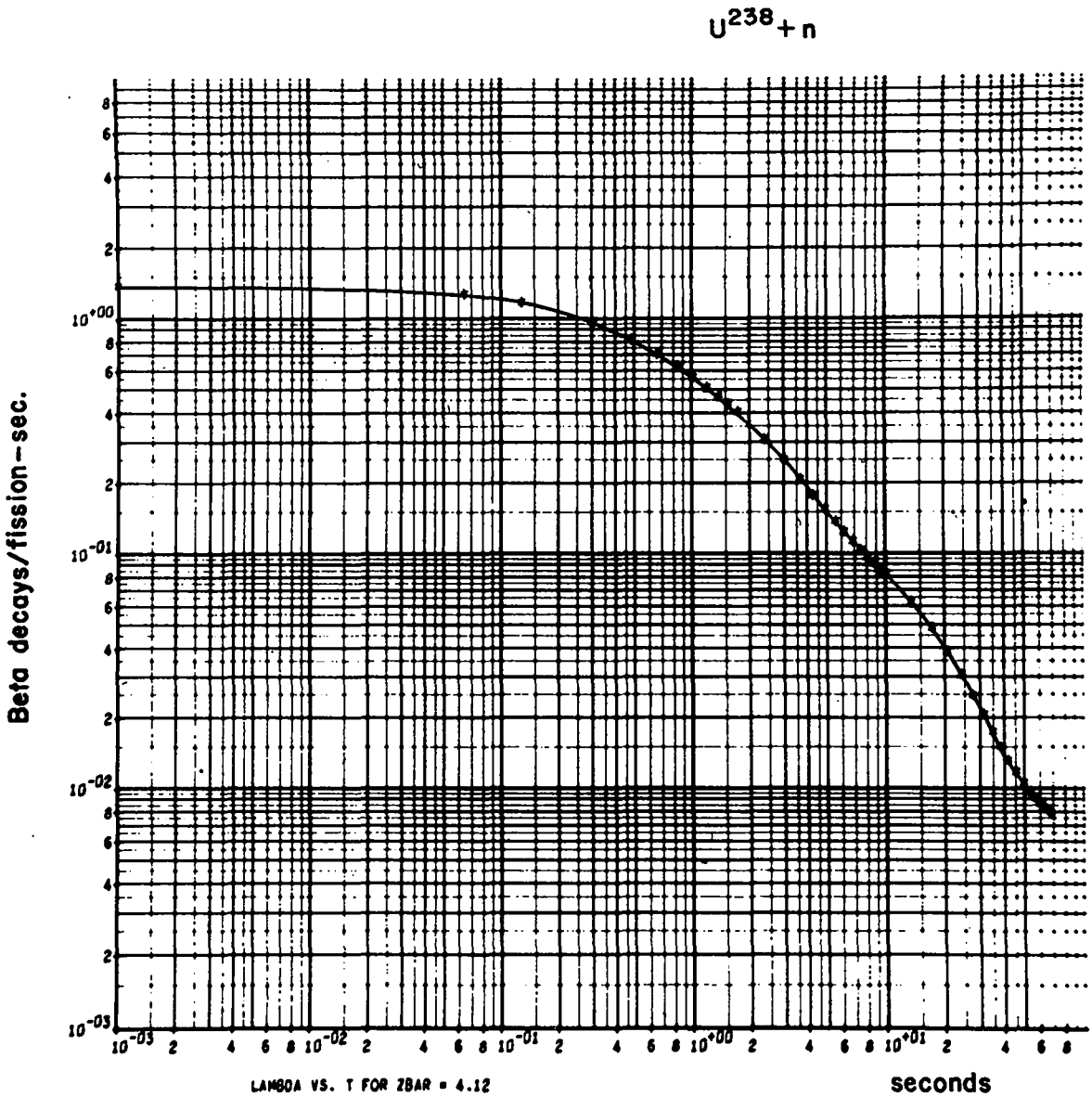

Fig. 11. Beta-Decay Rate for U^{238} + n vs. Time

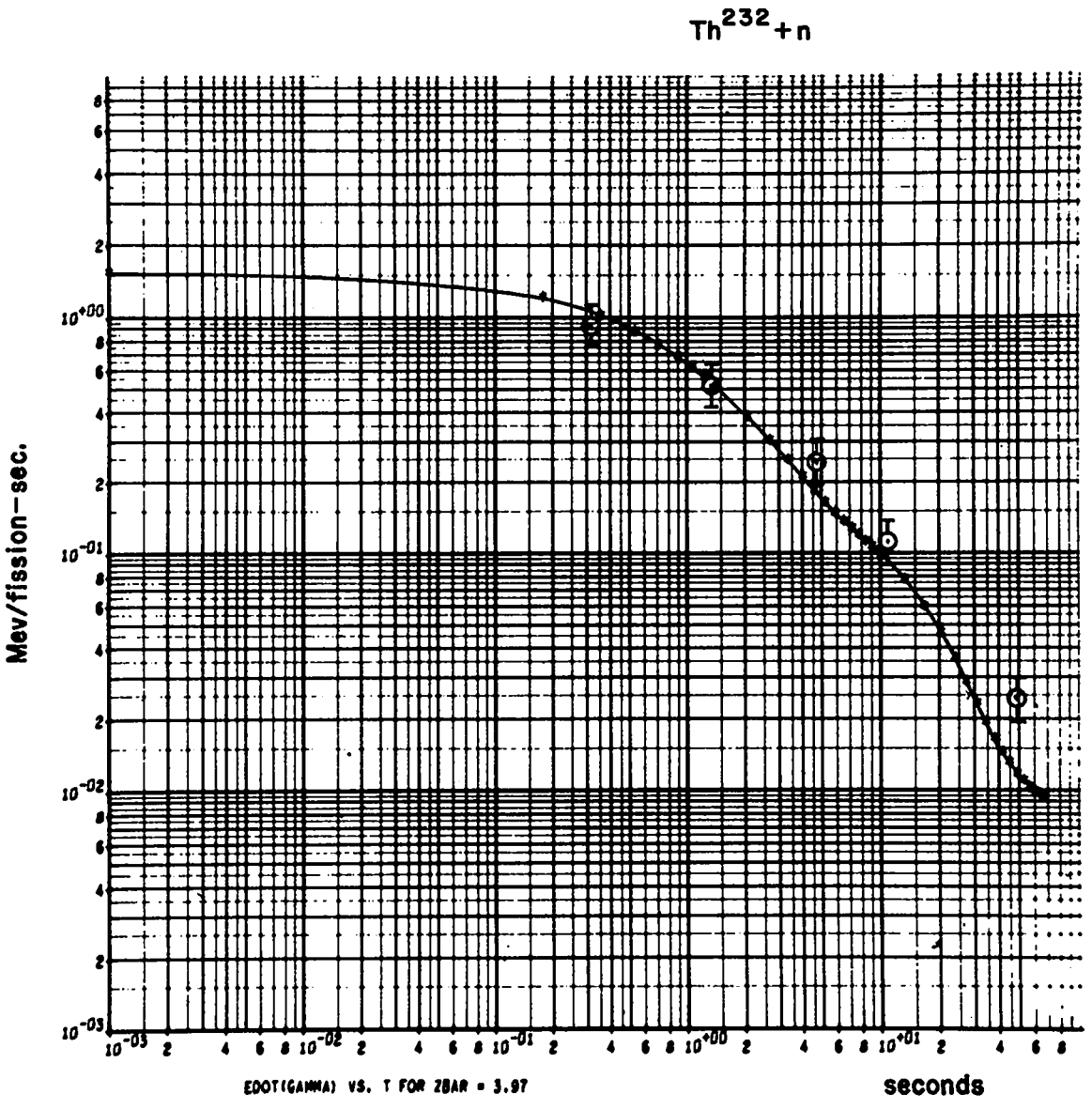

Fig. 12. Gamma Rate for Th^{232} + n vs. Time

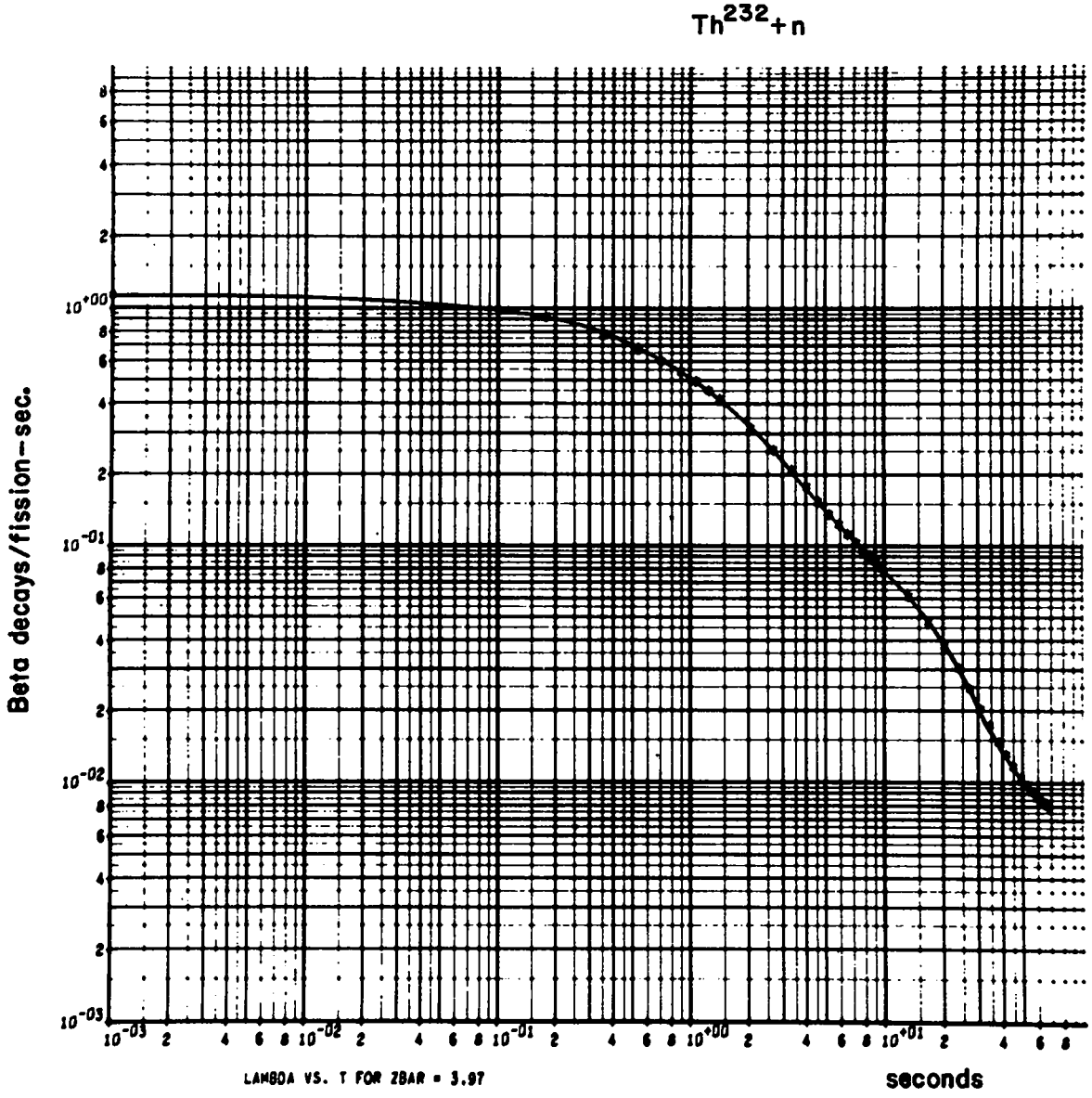

Fig. 13. Beta-Decay Rate for Th^{232} + n vs. Time

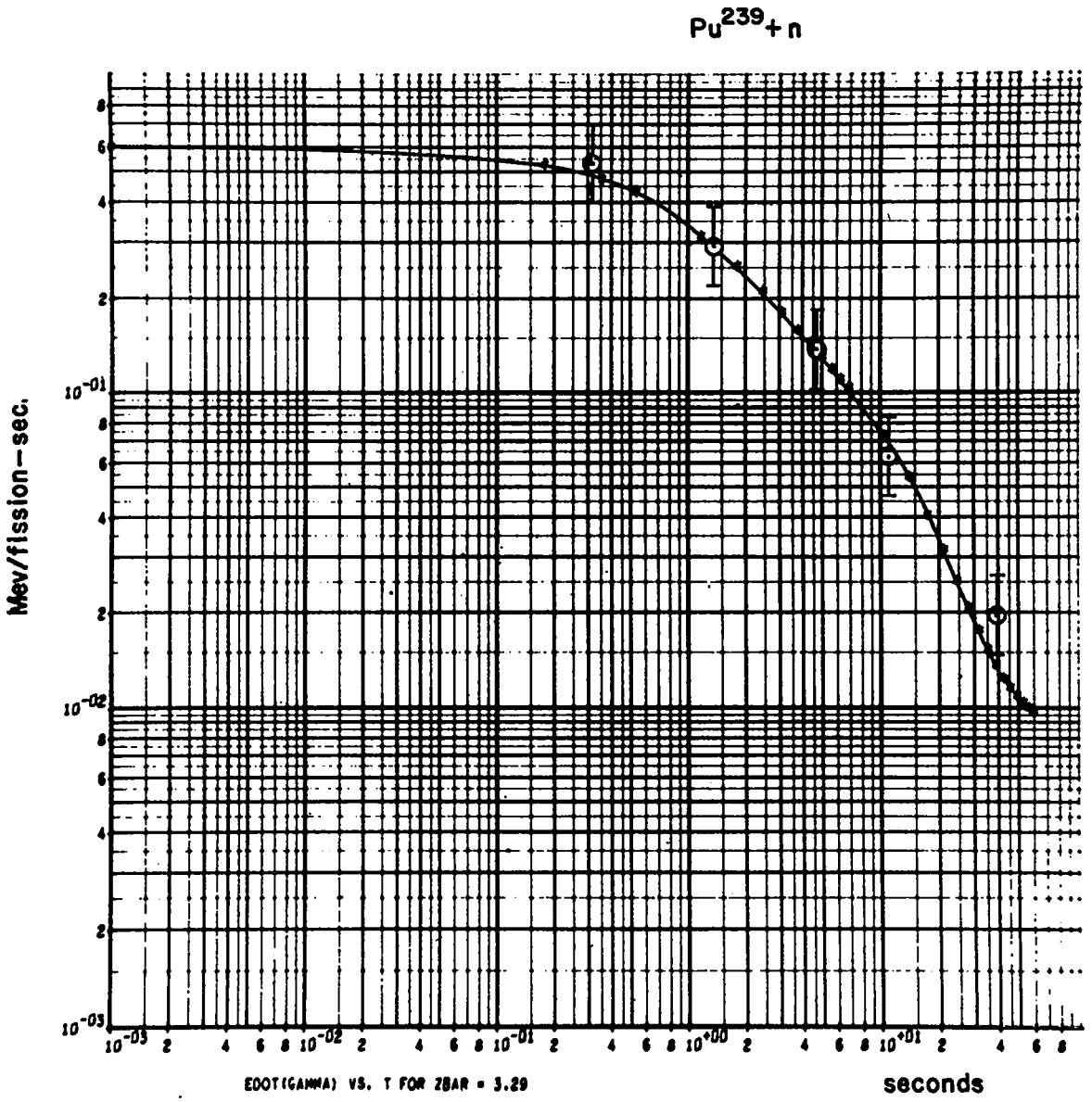

Fig. 14. Gamma Rate for Pu^{239} + n vs. Time

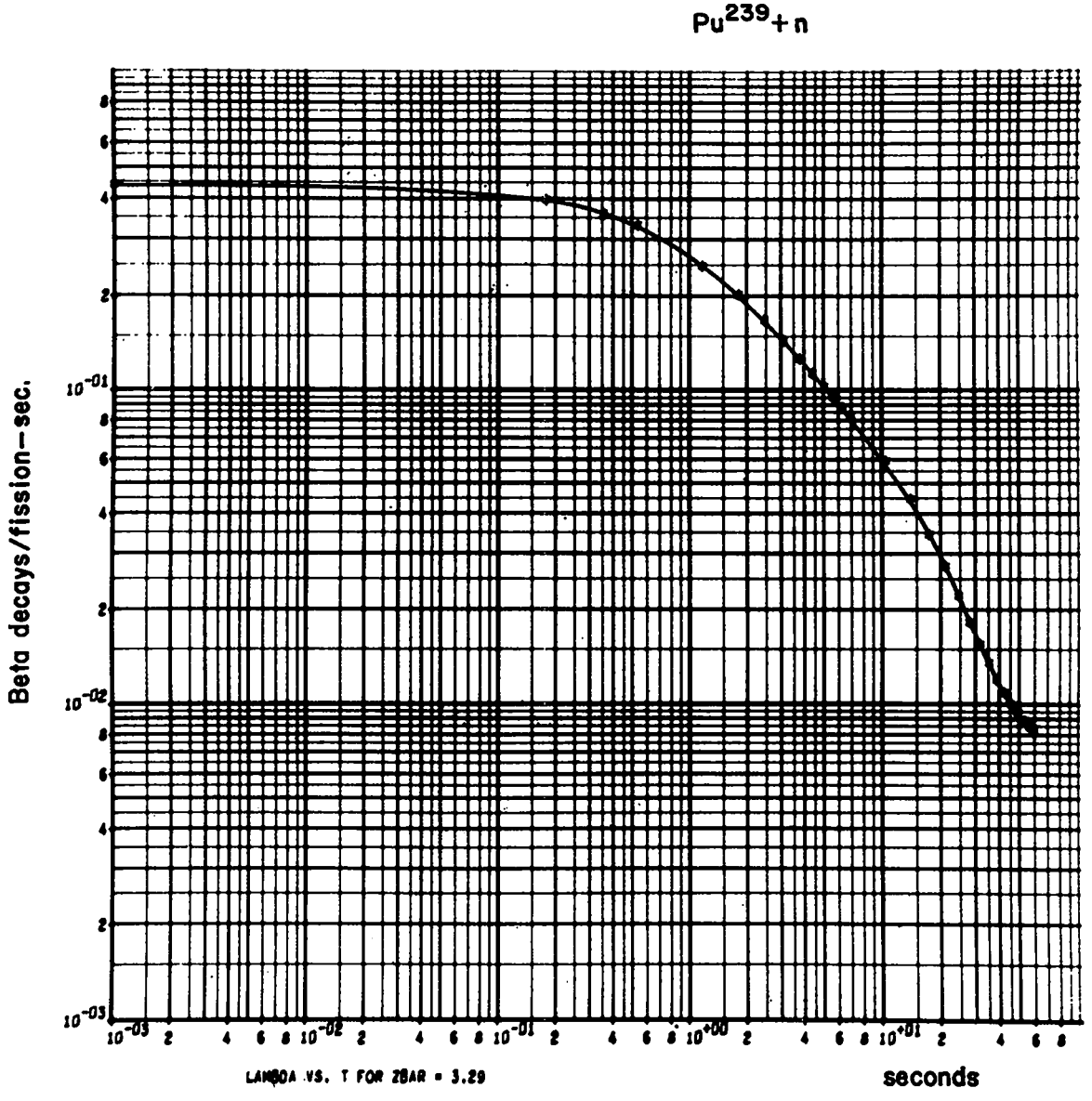

Fig. 15. Beta-Decay Rate for Pu^{239} + n vs. Time

REFERENCES

1. Maienschein, Peele, Zobel, and Love, Proc. U. N. Intern. Conf. Peaceful Uses At. Energy, 2nd, Geneva, Vol. 15, p. 366 (1958).

2. R. B. Walton, General Atomic Div., General Dynamics Corp., Air Force Report SWC TR-61-10 (1961).

3. S. Katcoff, Nucleonics 18, No. 11, 201 (1960).

4. Nethaway, Washington University thesis, as quoted by E. Hyde, University of California Radiation Laboratory Report UCRL-9036 (1960).

5. E. Fermi, Nuclear Physics, University of Chicago Press, 1949. The fact that this approximation is limited to values of $w(z) \geq 5\ mc^2$ is discussed in Section I.

6. B. R. Mottelson, The Many Body Problem, p. 283, John Wiley and Sons, New York, 1959, discusses the pairing model for nuclei, as does S. T. Belyaev (same reference, p. 343). The author is grateful to Dr. Mottelson for his helpful clarification of this aspect of the problem.

7. A. E. S. Green, Nuclear Physics, McGraw-Hill Book Co., New York, 1955.

8. L. B. Engle and P. C. Fisher, Los Alamos Scientific Laboratory Report LAMS-2642 (January 1962).

9. P. Armbruster and H. Meister, to be published.

10. E. Feenburg and G. Trigg, Rev. Mod. Phys. 22, 399 (1950).

11. The various data used in composing this table and references to the original measurements may be found in R. B. Leachman, Proc. U. N. Intern. Conf. Peaceful Uses At. Energy, 2nd, Geneva, Vol. 15, pp. 229 and 331 (1958).

12. R. B. Leachman, Phys. Rev. 101, 1005 (1956).

13. The author is grateful to Dr. James Terrell of this Laboratory for his helpful comments on this point.

14. J. F. Perkins and R. W. King, Nucl Sci. Eng. 3, 726 (1958).